

Modeling of Motor Starting Methods in EMTP-ATP

by Delcho Penkov, Motor Management Leader
Zhimin QIN, Verification Engineer
Weisheng Wang, Solution Architect
Jérôme Guillet, Motor Management Expert

Executive Summary

The work described in this paper has been developed for the purposes of medium voltage motor starting analysis in customer projects. EMTP-ATP today offers highly advanced modeling capabilities for motors and starting equipment. This paper will present models for several increasingly complex motor starting methods, such as direct on line (DOL), star-delta, wound rotor resistance, autotransformer, soft starter, and variable speed drive (VSD) with synchronous bypass.

Introduction

Motor starting is one of the key analyses necessary to validate the integration of a motor in an electrical installation. Such analyses can often be omitted, particularly when the motor involved is of low power or remains below 10% of the transformer or generator.

However, if the motor power is higher, then analyses, typically by simulation, will be necessary in order to define the most economic and convenient manner to start for the system and parallel loads. The main motor starting methods are well known and most of them have been widely discussed and presented in previous papers^{1, 2, 3}.

In this paper the authors review the different starting methods, focusing on the specific modeling challenges encountered in EMTP-ATP, and compare the performance of each method in a case study.

Typical Constraints for Motor Starting in Industrial Systems

Motor starting impacts three main elements: the industrial system, the driven load, and the motor itself.

Voltage drop during starting is the main impact on the industrial system. It is produced by the current drawn by the motor and is relative to the short-circuit impedance of the system. A higher impedance is characteristic of a power system with lower short-circuit power. Consequently, it will produce a higher voltage drop. Voltage drop up to 15% is usually acceptable but lower values are preferable.

The driven load is mainly impacted by the intensity of the start or the applied torque. Some high inertia loads like fans, or specific applications like water pumps, will suffer a sudden application of high torque, which may result in a high torsional effect or water hammer. In such cases, progressive starting is recommended.

The motor is impacted through mechanical stress, starting duration, and heating. It is recommended that thermal stress is limited to 80-90% of the motor thermal capacity to avoid premature aging.

¹J. Nevelsteen, H. Aragon, Starting of Large Motors - Methods and Economics, IEEE Transactions On Industry Applications, Vol. 25, No. 6, November - December 1989

²J. Larabee, B. Pellegrino, B. Flick, Induction Motor Starting Methods and Issues, in proc. of PCIC Conference 2005

³S. Rusnok, P. Sobota, V. Mach, P. Kacor, S. Misak, Possibilities of Program EMTP – ATP to Analyze the Starting Current of Induction Motor in Frequent Switching, EPE Conference 2015

Case Study for Comparative Analysis

A case study has been defined in order to compare the performance of the various starting methods.

General Data

The electrical network is composed of a power source with limited short-circuit power, power transformer, motor cable, and the motor. Details are provided in **Table 1**.

Table 1

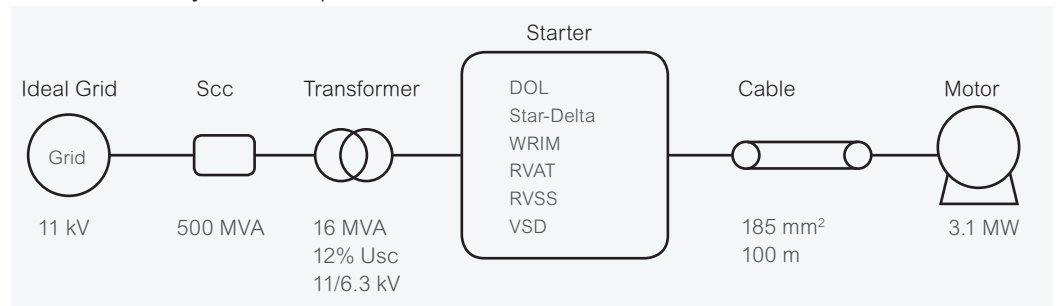
Case Study Equipment Characteristics

Equipment	Technical Characteristics
Upstream network	11 kV, 500 MVA
Power transformer	Dy11, 11-6.3 kV, 16 MVA, 12% Usc
Cable	Single core, 185 mm ² , 100 m
Motor & load	Pump, 3.1 MW, 6.3 kV

Figure 1

Principle of the Studied System

The electrical system is represented as:



Modeling the Motor and Load

The motor and load have been modeled using UM3 model, without saturation, with the following arrangement:

Figure 2

(A) Motor Diagram
(B) Compressed View of Motor and Load

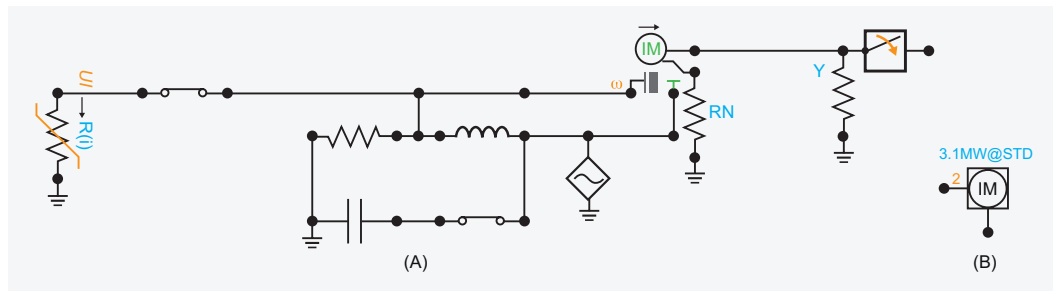


Table 2

Motor Datasheet Data and Resulting EMTP-ATP Model

The motor model has been defined as a best fit to match most datasheet performance values. The results are shown below in **Table 2**.

Characteristic	Datasheet Value	EMTP-ATP Model
Rated power (MW)	3.1	3.1
Rated voltage (kV)	6.3	6.3
Rated current (A)	320	310
Rated speed (rpm)	1489	1483
Rated torque (Nm)	19735	19735
Slip (%)	0.73	1.1
Starting current (pu)	5.6	5.6
Starting torque (pu)	0.7	0.615
Maximum torque (pu)	2.5	2.51
Power factor	0.92	0.94
Efficiency	96.7	97
Rs (Ω)	0.06	0.12
Rr (Ω)	0.17	0.21
Xm (Ω)	51.36	62.8
Xs (Ω)	1.453	1.522
Xr (Ω)	0.4622	0.4622
Motor & pump inertia (kgm^2)	219.4	219.4

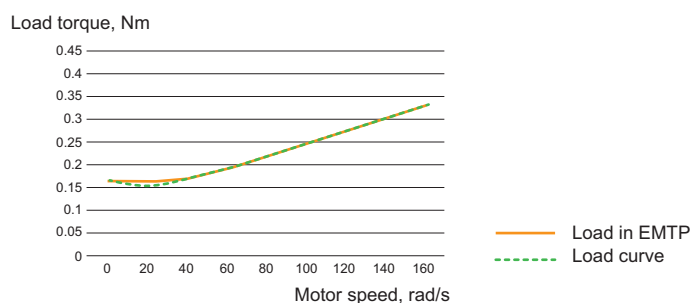
This best fit has been achieved through a simulation trial and error approach. The lack of saturation modeling will generally increase the maximum torque crest with speed,⁴.

The motor is originally designed in star connection. When the starting modes require the motor to be designed in delta connection, or to be wound rotor, the motor model has been transformed accordingly, always keeping the same electro-mechanical behavior.

The motor load is a pump. It has been modeled using the nonlinear current-dependent resistor TYPE 99. The load curve has a parabolic evolution, however, in EMTP-ATP it is necessary to define a monotonically increasing curve, which produces a more conservative curve.

Figure 3

Load Torque



Although in practice each starting mode and motor will be designed for a specific load, in this paper, for comparison purposes, the same load has been used for all starting modes and motors.

⁴ G. J. Rogers, D. Shirmohammadi, Induction Machine Modelling for Electromagnetic Transient Program, IEEE Transactions on Energy Conversion, Vol. EC-2, No. 4, December 1987

Modeling and Analysis of Motor Starting Methods

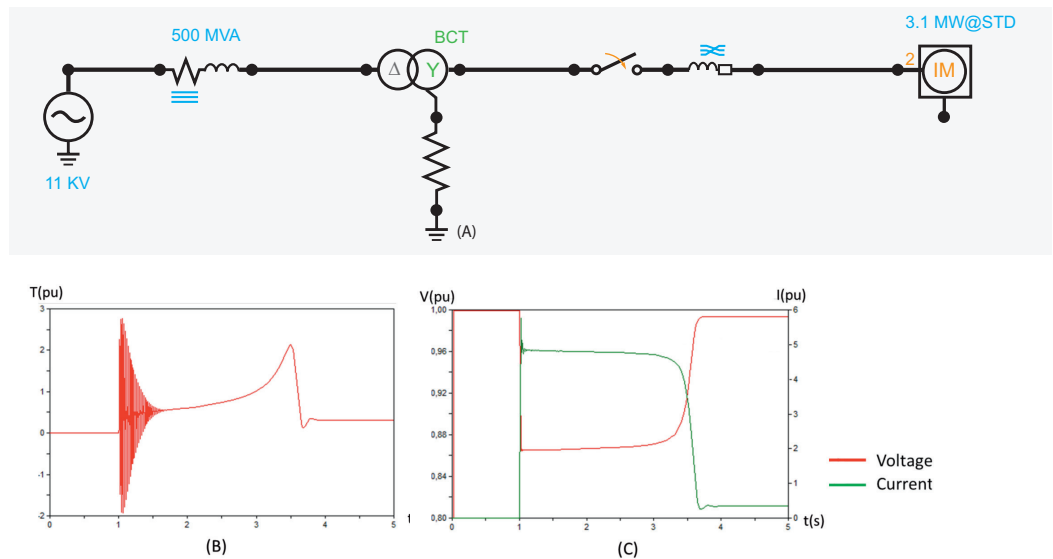
The focus on the results presented in this paper will be on motor torque evolution and transients, network voltage, and network current fed to the starter. For autotransformer starting, the current on the motor side will also be presented.

Direct On Line Starting

Direct on line (DOL) starting is the simplest and most economical way to start an induction motor, but it causes a considerable starting current, almost 5 to 7 times the rated current. In practice, a DOL start is achieved using a contactor or circuit breaker. In EMTP-ATP it is modeled by a 3-phase switch. The corresponding model and results are shown in **Figure 4**:

Figure 4

(A) DOL Starting Model
 (B) Motor Torque
 (C) Network Voltage and Current.



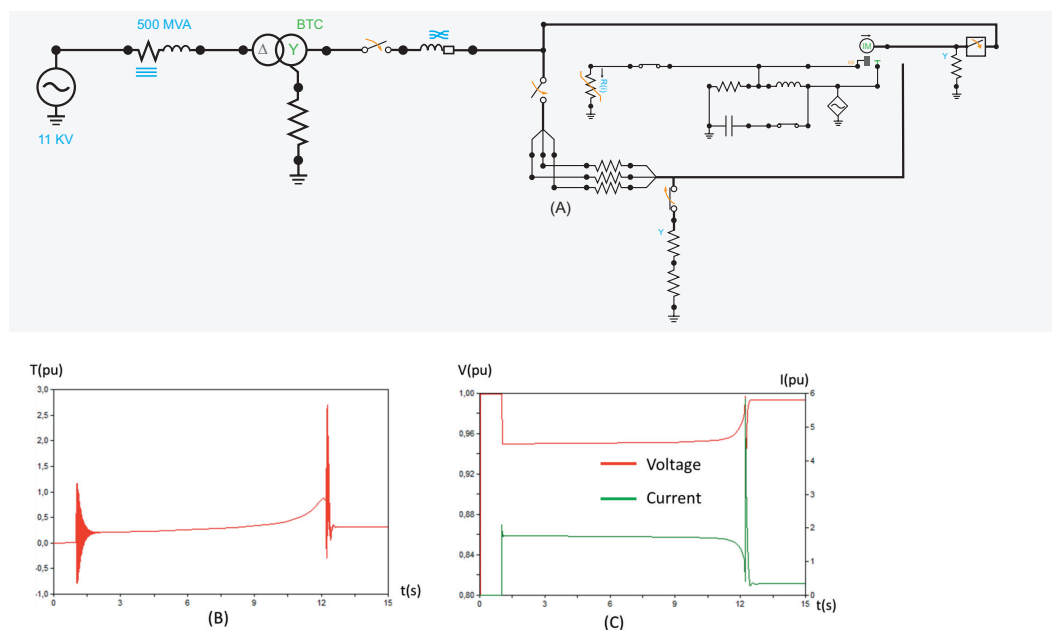
The results obtained show expected torque oscillations and a significant voltage drop (15%).

Star-Delta Starting

This is a very economical starting method that reduces the starting current. The equipment normally consists of three contactors and the motor must be designed in delta connection. The starting current is about one third of the direct on line start, as shown in **Figure 5**. (B). However, the process of switching from star to delta connection generates a significant oscillation torque.

Figure 5

(A) Star-Delta Starting Model
 (B) Motor Torque
 (C) Network Voltage and Current



Although the oscillation might be exaggerated in the simulation, it shows that this starting method produces high mechanical stress on the motor and may require more frequent motor maintenance. In practice, the star-delta method is reserved for infrequent starting and for smaller and inexpensive motors.

Wound Rotor Induction Machine Resistance Starting

This method is used when high starting torque has to be applied on the load and allows the starting current to be maintained at a relatively low value. It is used for starting constant torque loads such as conveyors or extruders. The high torque is obtained by connecting resistors on the rotor winding. Hence this method is used with wound rotor induction motors (WRIM). However, it does present some major drawbacks in terms of torque variation during starting and efficiency. In addition, the starter requires frequent maintenance. Nowadays, it is frequently replaced by a squirrel cage motor coupled with a variable speed drive⁵.

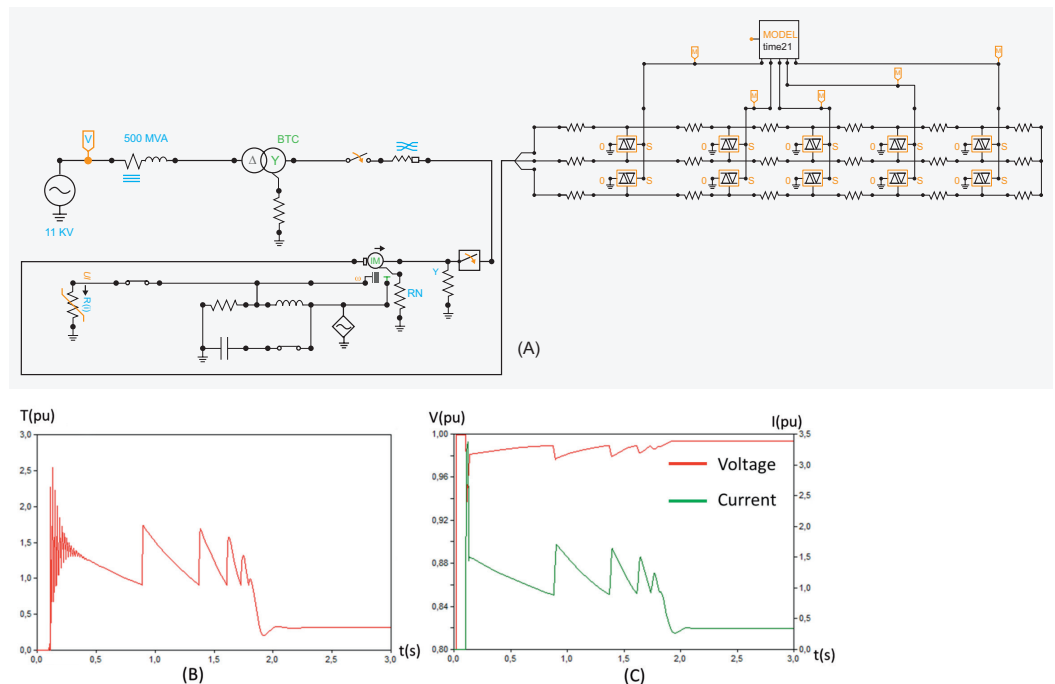
For the purposes of analysis, the UM3 motor model has been converted to UM4, using the same impedances. Although such a straightforward conversion does not reflect the change between the two motor technologies, it does allow us to make a better comparison of the performance of this starting method versus the others.

The resistance is controlled using a triac model TYPE 12 switch and a control logic block in MODELS. The principle is to measure the motor current and to close a bypass switch when the currents falls below a threshold value. For the case study, the threshold was set to $1.1 \times I_n$, roughly corresponding to a torque of the same ratio to rated.

Starting resistances were calculated⁵, as 0.173 Ω , 0.372 Ω , 0.8 Ω , 1.715 Ω , 3.7 Ω .

Figure 6

(A) Wound Rotor Induction Machine Starting Model
(B) Motor Torque
(C) Network Voltage and Current



As can be seen in **Figure 6**, each time a bypass switch is closed, there is a jump in the motor current and torque. Compared to previous methods, starting time is reduced and the voltage drop is also limited.

⁵Fahai L. 电机与拖动基础第三版 (Motor and drag), 2005

Autotransformer Starting

An autotransformer start, also called RVAT (Reduced Voltage Autotransformer), is another starting method that reduces the starting current, as the voltage across the motor is reduced during starting. The torque is reduced as the square of the applied voltage. When the motor has almost reached its rated speed, the motor is progressively connected in direct on line.

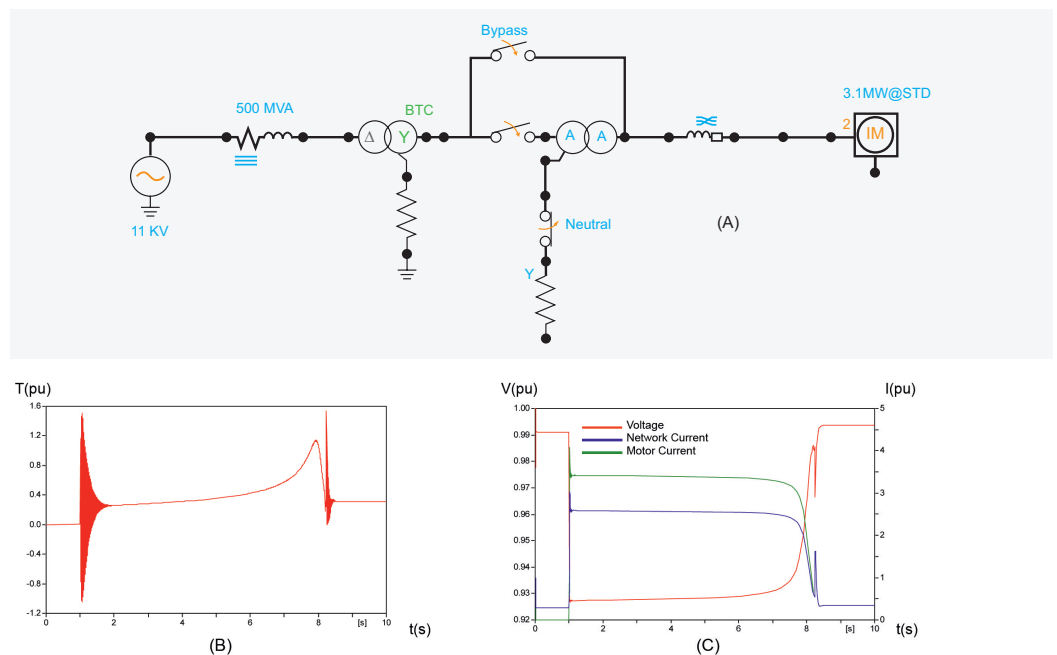
Three main steps are considered in this case. In the first step, the motor is connected to the starting voltage with autotransformer. The autotransformer neutral is then opened and the motor is connected to the network through the autotransformer impedance. In the last step, the motor is connected in direct on line.

Autotransformers have a different design from standard transformers, mainly in order to control the series impedance in the second step. Air-gaps are integrated in their magnetic circuit, which are calculated with reference to the expected current in the second step.

As a consequence, the losses of these transformers are higher as is their no-load current. **Figure 7** shows the autotransformer starting circuit in ATPDraw and the results from the simulation.

Figure 7

- (A) Autotransformer Starting Model
- (B) Motor Torque
- (C) Network Voltage and Currents



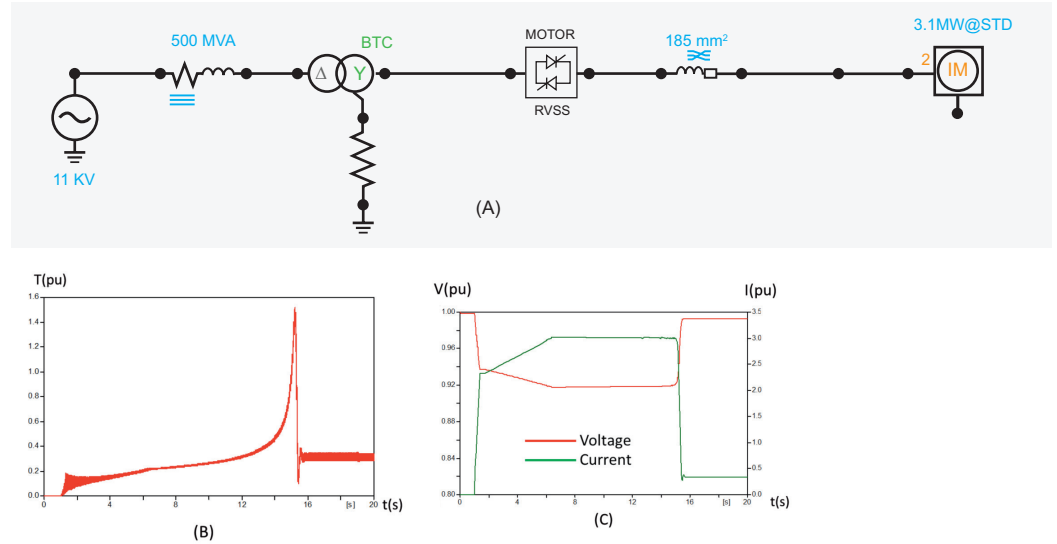
Due to the limited current, the motor takes longer to accelerate to full speed. In the transition from step 1 to 3, it is predominantly torque oscillations that are observed, which last much longer than those of current and voltage.

Soft Starter Modeling

The soft starter model, also called RVSS (Reduced Voltage Soft Start), has already been discussed in a previous contribution⁶. For the simulation, the soft starter has been set with 40% initial voltage roughly $2.2 \times I_n$, 5s ramp, and a current limit of $3 \times I_n$. The electrical network and results are shown in **Figure 8**:

Figure 8

(A) Soft Starter Model
(B) Motor Torque
(C) Network Voltage and Current



The current ramp and limitation phase can be clearly observed in **Figure 8**.

The voltage is evolving in the opposite manner. This is due to the constant impedance of the source. In the case of a generator, the voltage profile will change and the steady voltage drop will be limited through the voltage regulation. As expected, the motor torque has a smooth increase during the ramp time.

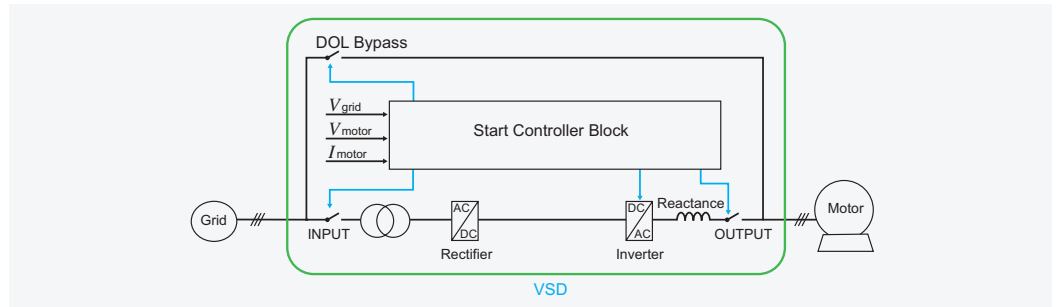
⁶ T-T-H. Pham, D. Penkov, S. Heighington, using EMTP/ATP for transient and stability analysis of an energy efficient LNG ship power system, EEUG Meeting 2015

Variable Speed Drive Modeling

With a variable speed drive, the speed of the asynchronous motor is controlled and, compared with other methods, it has the smallest starting current but a considerable starting torque. However, this starting equipment is the most expensive and complex of all the methods reviewed in this paper. When the drive is used for starting only, there is a parallel bypass device that connects the motor in direct on line once the start is finished.

The architecture of the VSD model, as shown in **Figure 9**, includes the rectifier, inverter, and controller:

Figure 9
Principle of Starting Using a VSD and a Bypass Contactor



Start Controller Block

This control block manages motor starting as well as the synchronization and transfer of the motor in direct on line connection.

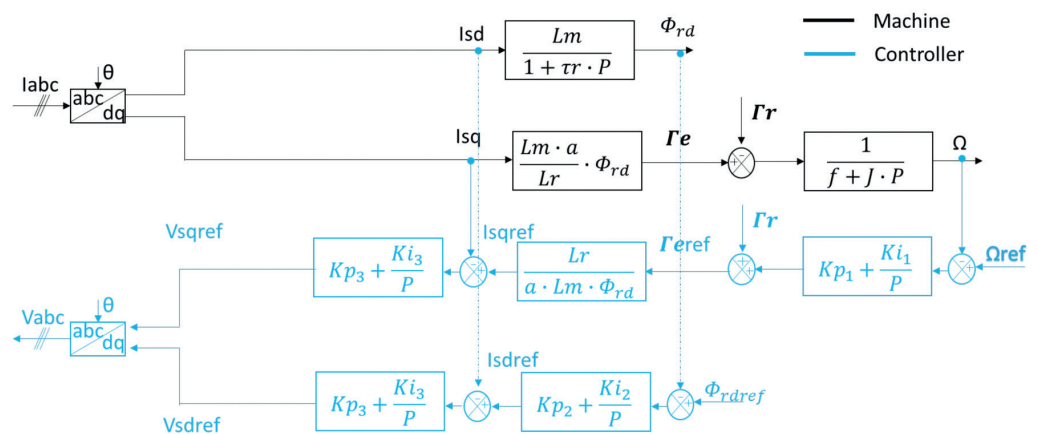
Vector Control Implementation

Motor starting is achieved using vector control, which gives better performance in terms of high torque at low frequency and better dynamic response.

However, it is also more sensitive to the accuracy of the motor input parameters, meaning that applications with double cage or deep bar rotors will require a dedicated dynamic motor parameters estimation routine.

In order to develop vector control, rotor flux oriented coordination transformation was selected. **Figure 10** shows the block diagram for the equivalent motor model and its relation with the developed vector control. The PI controller parameters and variable denominations are provided in the appendix.

Figure 10
Vector Control Block Diagram



Bypass System and Synchronization

The bypass system allows motor operation across the line. One contactor is installed between the incoming line and the VSD input (input switch), and a bypass contactor is installed between the incoming line and the motor (DOL switch). A third contactor is installed between the VSD output and the motor (output switch) as shown in **Figure 9**. A synchronization reactor is installed at the VSD output to limit the fault current. The reactor in this particular case has a value of 0.4 mH.

Once the motor reaches a reference speed, the control is switched to scalar control and the voltage on the motor side is smoothly aligned with the network voltage. The bypass switch is then closed and the VSD is progressively disconnected from the network.

Cascaded H-Bridge Multilevel Inverter and Rectifier

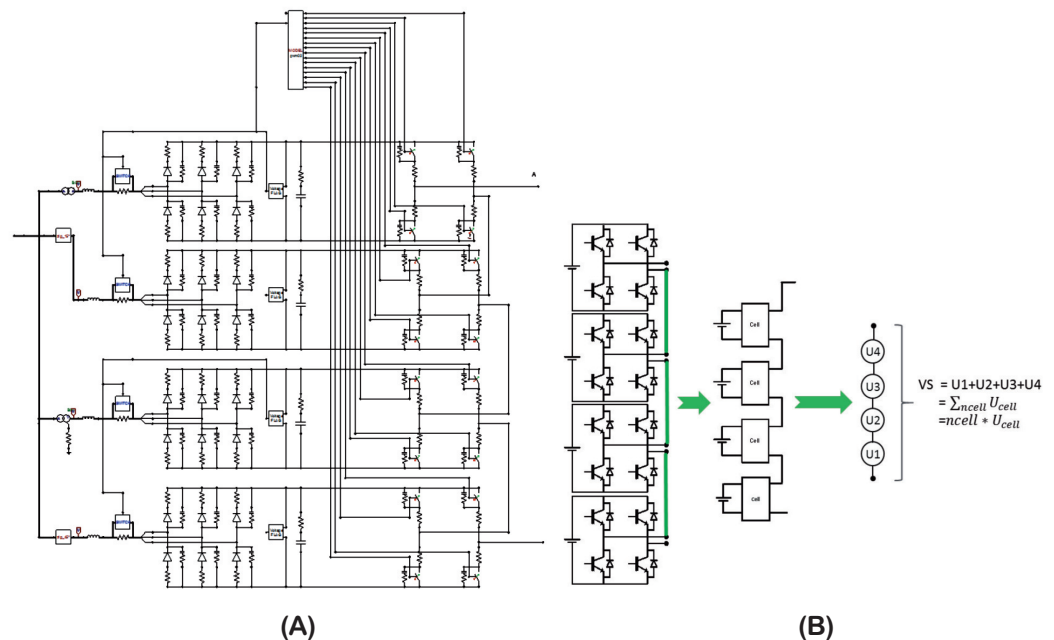
Since the traditional two-level inverter cannot be effectively applied to the field of high voltage and medium voltage frequency control, a multilevel conversion technology has been introduced. There are many types of multilevel inverter, including: NPC (neutral point clamped) inverters, imbricated cell multilevel inverters, and cascaded inverters.

A cascaded H-bridge inverter was considered for the purposes of this paper because of the advantages it offers, such as low switching stress, high quality load wave, simple algorithm, easy packaging, and high equivalent switching frequency. The use of cascaded inverters is becoming increasingly popular in variable frequency speed regulation systems⁷.

A cascaded inverter is composed of several power cells. Each power cell has its own DC power, produced by a multi-pulse rectifier. **Figure 11** illustrates the topology of a single-phase cascaded inverter. It is made up of 4 cells and the output waves are $2n+1$, or 9 levels. These multiple levels of voltage, hence power cells, help to reduce the output harmonics and increase the equivalent switching frequency⁸. This higher switching frequency means that the oscillation torque is also reduced. Respectively, the higher number of power cells means that the input rectifier is also of a higher level. The harmonic currents on the network side are also reduced through an appropriate coupling of the secondary windings on the input transformer⁹. There are 4 secondary windings in the model presented below. The phasing is obtained using zigzag transformers. It is worth mentioning that the input transformer model varies from an actual transformer in that it does not consider mutual impacts from secondary windings, given that it has an individual primary winding for each.

Figure 11

(A) Cascaded H-Bridge Multilevel Inverter Model
(B) Topology



⁷ ZHANG Jingjun, H 桥级联型多电平逆变器的研究 (Cascaded H-bridge multilevel inverters research), 2011

⁸ 江友华 (JIANG Youhua), 曹以龙 (CAO Yilong), 龚幼民 (GONG Youmin), 基于载波相位移角度的级联型多电平变频器输出性能的研究 (Research on Output Performance of Cascaded Multi-level Inverter Based on Carrier Phase Shift Angle), 中国电机工程学报 (Journal of China Electromechanical Engineering), 76-81, 2007

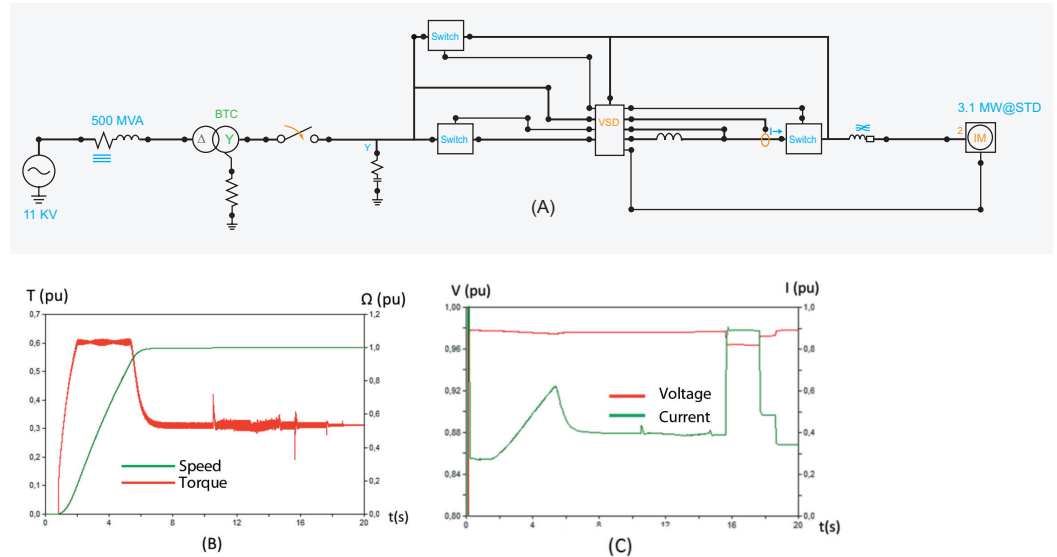
⁹ WANG Zhaoan 王兆安. (n.d.), 电力电子技术 (第四版) (Power Electronics).

Simulation Results

For motor starting, the torque is set to 60% of the rated value. Once the motor is close to rated speed, the synchronization sequence is initiated. **Figure 12** illustrates the model obtained in ATPDraw and the starting results:

Figure 11

(A) VSD Starting Mode
(B) Motor Torque and Speed
(C) Network Voltage and Current



The results show very short and limited transients in the torque, at the change of the control type and at the closing of the bypass contactor. During parallel operation in direct on line and VSD mode, the consumed current is higher.

The motor consumption remains unchanged, but the variable speed drive and bypass switch form a current loop and there is a consumption of reactive power.

When the VSD is stopped, the loop is opened and the consumed current from the network and that of the motor become equal.

Summary of the Analyses

Table 3

Summary of the Motor Starting Results with Different Starting Methods

The simulation results are presented in **Table 3**:

Characteristic	DOL	Star-delta	WRIM	RVAT	RVSS	VSD
Starting time (s)	3.9	13	2.2	7.5	15.2	18.9
Starting current (pu)	4.88	1.77	3	3.42	3	<1
Voltage drop (%)	15	5	<2	7.6	8	<2
Starting torque (pu)	0.55	0.2	1.7	0.27	0.11	0.6
Motor heating (%)	22.6	14	<1	31	46	<1

From the results shown above, it can be concluded that longer acceleration times are obtained with progressive starting methods, such as star-delta, autotransformer and soft starter, where the motor torque is reduced. Generally, longer starting times mean also higher motor heating, except in the star-delta method where reduction in current is higher than the increase in starting time. Motor torque is higher with rotor resistance starting and variable speed drive. Voltage drop is exhibited most predominantly in direct on line starting, with all other methods being very efficient in reducing the voltage drop below 10%.

Conclusion

Several motor starting methods are modeled and compared in this paper. These models are intended for use in real projects for evaluating appropriateness of a given starting method, or to be used as a basis for reference for developing simplified comparison tools for non EMTP-ATP users. During the development of the models, some EMTP-ATP limitations have been identified, including the difficulty of fitting the motor model to datasheet data, and autotransformer operation with an open neutral.

However, in the majority of cases, EMTP-ATP and ATPDraw have allowed an easy model implementation, and the results obtained match the expected behavior for the various motor starting methods.

About the Authors

Delcho PENKOV graduated from the Technical University of Sofia, Bulgaria, in 2002 with an engineering degree. In 2006 he obtained his PhD in electrical engineering from the Institut National Polytechnique in Grenoble, France. He started his career at Schneider Electric as a technical expert for transient analysis and simulation. He is currently leading the Motor Management Competency Center for high-power motor applications. He has authored and co-authored several papers and patents for motor application oriented equipment. He is a member of the IEEE and European EMTP-ATP Users Group.

Zhimin Qin graduated from the Institut National Polytechnique de Grenoble in 2017. He is currently a validation engineer, based in Shanghai.

Jerome Guillet graduated with a Master's degree in mechanical and industrial engineering from the Arts et Métiers ParisTech in 2004. He started his career at the electrolytic capacitors manufacturer SICSAFCO as a technical engineer in 2005. He joined Schneider Electric Power Quality as an R&D engineer in 2008. Since 2015, he has worked in the Motor Management Competency Center. He currently assists during the early stages of large motor projects, and contributes to popularize motor knowledge with dedicated calculation tools and training.

Wang Weisheng was born in Gansu, China in 1983. He graduated with a Bachelor degree from Tongji University in 2005. He is now employed by Schneider Electric as a solution architect implementing drive application solutions. His specialist field of interest is synchronous motor control.



Annex

Appendices

Denominations of variables used in vector control:

P	Laplacian operator
L_r	Rotor inductance
L_m	Mutual inductance
τ_r'	L _r /R _r (rotor resistance)
a	Number of pole pairs
f	Coefficient of friction
J	Inertia
Φ_{rd}	Rotor flux in D axis

Values of the PI regulators for vector control

Parameter	Value
K_{p1}	1948.5
K_{i1}	3897
K_{p2}	300
K_{i2}	312.7
K_{p3}	19.2
K_{i3}	360



Contact us

For feedback and comments about the content of this white paper:
motor.management@schneider-electric.com

Schneider Electric Industries SAS

35, rue Joseph Monier - CS 30323 - 92506 Rueil Malmaison Cedex - France

© 2018 Schneider Electric. All rights reserved.

998-2095-11-08-18AR0_EN

www.schneider-electric.com